THE ASTRONOMICAL JOURNAL VOLUME 99, NUMBER 1 JANUARY 1990

THE RADIO PROPERTIES OF cD GALAXIES IN ABELL CLUSTERS. I. AN X-RAY-SELECTED SAMPLE

JACK O. BURNS[a),b)]
Institute for Astrophysics, Department of Physics and Astronomy, The University of New Mexico, Albuquerque, New Mexico 87131
Received 15 May 1989; revised 10 July 1989

ABSTRACT

The radio and x-ray properties of a sample of 27 cD galaxies in rich clusters are presented in this paper. The radio data consist of 6 cm VLA maps at a resolution of 1–2 arcsec. The x-ray data consist of images and surface-brightness profiles from the *Einstein* IPC, and derived quantities such as cooling times, mass-accretion rates, and thermal pressures from Arnaud (1988). These data are used to explore the relationship between x-ray cooling cores, and the power and morphology of the radio emission. We find that 71% of the cD's with x-ray cooling cores are radio loud, whereas a smaller but still significant 23% of cD's without cooling cores are detected at 6 cm above 0.2 mJy. Among the radio galaxies in noncooling core clusters are luminous and extended wide-angle tails. There is a weak correlation between the mass-accretion rate and the radio power for cD's. There is also an interesting class of cooling core cluster (e.g., A2052) with small diameter, amorphous radio emission that may be the result of diffusion along radial magnetic fields set up in cooling inflows. Finally, we examine the relationships between optical emission-line luminosity with radio power and mass-accretion rate.

I. INTRODUCTION

Supergiant cD galaxies were first recognized as a separate class of elliptical galaxy by Matthews, Morgan, and Schmidt (1964). cDs are characterized by their extended optical envelopes (up to 1 Mpc diameter in some cases), their location at the centroids of galaxy surface-brightness enhancements (usually at the centers of clusters), and their high optical luminosity (typical $M_v \approx -23$). Even in 1964, the radio properties of cD galaxies drew considerable attention since Matthews *et al.* recognized this class of galaxy from their optical identifications of 3C radio sources. cD galaxies tend to be radio loud and radio luminous more often than typical nondominant cluster ellipticals (e.g., Burns, White, and Hough 1981; Valentijn and Bijleveld 1983). This is consistent with the bivariate radio luminosity function in which optical and radio luminosity are known to correlate (e.g., Auriemma *et al.* 1977). Both properties, however, may be a product of the unique environment and evolution of these supergiant galaxies at the cores of clusters (e.g., Tonry 1985; Merritt 1984; Begelman 1986).

The x-ray properties of cD galaxies and the surrounding clusters are also exceptional (e.g., Sarazin 1986; Jones and Forman 1984; Fabian 1988). cD clusters tend to be the most x-ray luminous class of cluster (10^{44-45} ergs/s between 2 and 10 keV). They tend to have small core radii (< 300 kpc), as determined by fits of the surface-brightness profiles to bounded isothermal sphere models. The x-ray emission is always centered on the cD suggesting that the supergiant galaxy lies at the heart of the gravitational potential well. These properties led Forman and Jones (1984) to classify these clusters as XD (x-ray dominant) and to speculate that a substantial fraction of these clusters are dynamically evolved. One-third of the Forman and Jones sample contain clusters with central radiative cooling times less than a Hubble time. These "cooling cores" are directly observed near the centers of a few clusters from spatially resolved x-ray iron-line measurements (e.g., Mushotzky *et al.* 1981; Canizares *et al.* 1982). As the central gas cools, the pressure at the core drops. According to the now standard model (see, e.g., Sarazin 1986), the higher pressure in the outer parts of the cluster will drive a flow into the cluster center. This produces an excess in the x-ray surface brightness in the center of the cluster in comparison to that interpolated from an isothermal hydrostatic model fit to the outer cluster (see Figs. 1–7).

The relationship between cooling cores and radio emission is somewhat contradictory. Forman and Jones suggested that there is a strong correlation between the presence of central galaxy radio emission and cooling cores in clusters based upon their *Einstein* x-ray sample and single-dish radio data from Owen *et al.* (1982). O'Dea and Baum (1986) find a weak correlation between the 20 cm radio power and the excess central x-ray luminosity in cooling core clusters. Valentijn (1988) finds a strong correlation between x-ray and radio luminosities for dominant cluster galaxies. On the other hand, Zhao, Burns, and Owen (1989) do not find as strong a correlation between radio emission and cooling core clusters based upon a sample drawn from their 20 cm VLA radio survey and the *Einstein* database. In particular, they note that one class of radio source associated with optically dominant cluster galaxies, wide-angle-tailed (WAT) sources, are found almost exclusively in clusters without cooling cores. The cloudiness of this issue regarding radio emission and cooling cores may originate in part from differences in source samples and the unfortunate incompleteness (see below) in the *Einstein* cluster database.

This paper is the first in a series that will examine the radio properties of the most optically dominant class of rich cluster galaxy, cD's, with reasonably high angular resolution (1–2 arcsec) and good sensitivity. The particular subsample of clusters reported in this paper was selected because of the high-quality x-ray analysis recently completed by Arnaud (1988). We discuss the radio and x-ray properties of 27 rich clusters with cD galaxies, of which 14 have purported cooling cores. This will provide yet another sample in which we can examine the relationship between radio emission and cooling cores. In Sec. II, the sample is described in more detail, the VLA observations and reductions are discussed, *Einstein* x-ray images are presented, and the properties of individual clusters are noted. In Sec. III, the radio morphologies of cD galaxies are classified, and relationships

[a)] Visiting Observer of the National Radio Astronomy Observatory which is operated by Associated Universities, Inc., by cooperative agreement with the National Science Foundation.
[b)] Present address: Astronomy Department, New Mexico State University, Box 30001/Dept. 4500, Las Cruces, NM 88003.

between inferred accretion infall rates with radio power and radio-source sizes are described. In Sec. IV, we discuss the possible origins of the cooling-core/radio correlation, ideas concerning jet disruption in transonic cooling inflows, and possible diffusion effects as an explanation for the outer amorphous radio emission in some cD galaxies.

II. OBSERVATIONS AND DATA ANALYSIS

a) The Sample

The parent sample of cD galaxies in rich clusters was chosen from the recently published list of cluster classifications by Struble and Rood (1987). We selected for observations with the VLA all Abell clusters that have cD galaxies listed as the first brightest member including all richness classes. Clusters of distance class 3 and closer were ranked first for observation, distance class 4 was second, and distance class 5 was third. With 24 hr of VLA time allocated to this project, nearly all priority 1 clusters were observed as were priority 2 and many priority 3. Approximately 100 cD galaxies were observed in all.

In order to provide accurate positions for pointing the VLA with relatively high resolution, we measured the optical centroid positions of the cD galaxies in our sample. The measurements, accurate to about 1″, were made with the NRAO Mann measuring engine at the VLA. Since these positions may be of use to other observers, we are providing a list of the new measured positions for the subsample described below in Table I. A few cD optical positions were taken from Tonry (1985).

Recently, Arnaud (1988) described a catalog of 106 clusters of galaxies observed by the *Einstein* x-ray telescope and analyzed in the most thorough fashion to date. Arnaud examined all the clusters observed by either the IPC or HRI detectors and selected those images with at least 300 counts, with circular symmetry, and without significant substructure. Unfortunately, this sample is not statistically complete but does represent the largest x-ray database for clusters defined as above. He then produced surface-brightness profiles of x-ray emission in these clusters. Using a deconvolution technique similar to that described by Fabian *et al.* (1981), Arnaud estimated the central cooling time, cooling radius (within which the cooling time is less than the Hubble time), and accretion rate. About 45% of the clusters examined have "cooling cores" (i.e., central cooling time is less than a Hubble time). Arnaud kindly provided to us his list of cluster x-ray properties prior to publication.

TABLE I. New optical centroid positions of cD galaxies.

Cluster	RA (1950)	Dec (1950)
A85	$00^{h}39^{m}18^{s}.66$	$-09^{\circ}34'40''.9$
A133	$01^{h}00^{m}15^{s}.42$	$-22^{\circ}09'18''.9$
A399	$02^{h}55^{m}08^{s}.74$	$+12^{\circ}49'49''.0$
A644	$08^{h}14^{m}59^{s}.26$	$-07^{\circ}21'22''.8$
A1650	$12^{h}56^{m}07^{s}.32$	$-01^{\circ}29'31''.1$
A1767	$13^{h}34^{m}20^{s}.30$	$+59^{\circ}27'38''.1$
A1795	$13^{h}46^{m}34^{s}.21$	$+26^{\circ}50'24''.9$
A1809	$13^{h}50^{m}35^{s}.51$	$+05^{\circ}23'43''.5$
A1890	$14^{h}15^{m}09^{s}.47$	$+08^{\circ}24\ 36''.4$
A2029	$15^{h}08^{m}27^{s}.47$	$+05^{\circ}55'57''.5$
A2107	$15^{h}37^{m}27^{s}.35$	$+21^{\circ}56'34''.2$
A2124	$15^{h}43^{m}05^{s}.72$	$+36^{\circ}15'53''.7$
A2244	$17^{h}00^{m}51^{s}.92$	$+34^{\circ}07'58''.9$
A2271	$17^{h}20^{m}54^{s}.07$	$+78^{\circ}04'00''.4$
A2319	$19^{h}19^{m}36^{s}.70$	$+43^{\circ}50'59''.7$
A2420	$22^{h}07^{m}38^{s}.19$	$-12^{\circ}25'02''.8$
A2593	$23^{h}21^{m}49^{s}.29$	$+14^{\circ}22'20''.2$
A2626	$23^{h}33^{m}59^{s}.53$	$+20^{\circ}52'07''.7$
A2670	$23^{h}51^{m}39^{s}.62$	$-10^{\circ}41'51''.6$

We cross correlated our parent sample with that of Arnaud to produce a list of 27 clusters that had been observed in common. Only one cluster that was listed by Arnaud as having a cD galaxy, A1644, was not observed by the VLA. This subsample, then, has the best x-ray and radio data for analysis of the gas properties of clusters with very dominant central galaxies.

b) VLA Observations and Reductions

The entire parent sample was observed in the VLA B configuration of 1986 September 7 and 13 with a "snapshot mode" at a wavelength of 6 cm and an effective bandwidth of 50 MHz. Integration time on each source was 5–10 min. This particular combination with average resolution of 1–2 arcsec was chosen so that we might resolve many of the compact sources known to be commonly associated with dominant galaxies from 20 cm surveys (Zhao, Owen, and Burns 1989), yet would have reasonable sensitivity to lower surface-brightness structures up to about 1 arcmin in diameter. This compromise meant, in some cases, that we would not be able to sample all the spatial frequencies associated with the larger sources. The 6 cm system had the lowest receiver temperature of the four receivers present on the VLA at the time of observation, allowing us to achieve typical rms noises of about 0.2 mJy.

The data were calibrated in the usual fashion using 3C 286 as the primary flux density calibrator on the Baars *et al.* (1977) scale. The resulting data from the VLA consisted of two independent pairs of circularly polarized visibilities. After editing out bad visibility points in each total intensity database, the data were merged into a single database. "CLEANED" maps were then made of these fields using the program "MX" within the NRAO AIPS computer package running on a VAX 8650 at the University of New Mexico. In several fields where bright point sources existed, several rounds of phase and amplitude self-calibration (e.g., Schwab 1980) were performed to improve the dynamic range. Also, in several fields, a "natural weighting" that emphasizes the more heavily sampled inner portion of the u − v plane at the expense of the longer spacings was applied to better map the extended features.

The results of these reductions are given in Table II and in Figs. 1–9.

c) X-Ray Data

For most of those clusters with resolved radio sources, we have also shown the distribution of x-ray emission and the x-ray surface-brightness profiles in Figs. 1–9. The x-ray data are from the *Einstein* IPC database (with the exception of PKS 0745 − 19, which is an HRI image). For each IPC field, the image was corrected for vignetting and an average background, determined away from the source, was subtracted in a procedure similar to that described by Jones and Forman (1984). The image was then convolved with a 2D Gaussian with 1.5 arcmin FWHM (approximate beam response of the IPC) to better illustrate extended structure.

The centroid of each x-ray source was determined, and the radial surface-brightness profile was constructed by azi-

TABLE II. Data on cD clusters

Cluster	X-ray (H_o = 50)					Optical (H_o = 75)			Radio (H_o = 75)					
	L_x ergs/sec	$\dot{M}$ M_o/yr	t_{cool}/t_{Hubble}	R_{cool} (kpc)	P_c $\times10^{-11}$dyn cm^{-2}	z	σ_R km/sec	L_{line} ergs/sec	P_{20} (W/Hz)	P_6 (W/Hz)	α	LLS (kpc)	P_{min} $\times10^{-11}$	Morph.
0745-191	45.25[1]	489	0.05	170	19.3	0.1028	830	42.11[12]	25.74[3]	24.90	1.36	2.4	125	Amorphous
A85	44.62	128	0.4	153	5.1	0.0518	1440	39.90[13]	23.43[2]	22.78	1.08	1.6	11.2	Amorphous
A133	44.38	87	0.4	160	1.9	0.0570	--	39.53[13]	23.92[5]	22.64[5]	2.82[5]	45	30.0	Amorphous
A399	44.37	--	4.8	--	5.0	0.0715	1424	--		<21.42	--	--	--	--
A401	44.93	12	1.0	54	3.9	0.0748	--	<39.34[13]		<21.70[4]	--	--	--	--
A496	44.36	101	0.1	168	1.4	0.0316	657	40.17[13]	23.10[2]	22.99	0.2	0.2	358	Point[2]
A644	44.90	326	0.5	246	2.4	0.0781	--	<39.45[13]	--	<21.43	--	--	--	--
A671	43.58	--	1.7	--	1.0	0.0497	--	--	--	<21.00	--	--	--	--
A1650		--	2.7	--	6.1	≈0.14	--	--	--	<22.05	--	--	--	--
A1767	44.49	43	0.7	142	1.2	0.0756	--	--	--	<21.39	--	--	--	--
A1795	44.71	294	0.2	215	4.5	0.0621	778	41.64[14]	24.91[7]	24.24	1.07	13	9.7	Bipolar
A1809	43.84	--	3.2	--	1.4	0.0788	--	--	--	<21.55	--	--	--	--
A1890	43.48	--	>1	--	1.0	0.058	--	--	--	<21.24	--	--	--	--
A2029	44.84	366	0.3	226	4.7	0.0767	--	<39.53[13]	24.85[7]	24.03	1.31	53[2]	13.3	Dual Jet
A2052	44.24	127	0.1	189	1.2	0.0345	576	40.23[14]	25.10[7]	24.33	1.23	39[2]	1.1	Amorphous
A2063	43.98	45	0.2	124	1.3	0.0337	521	<39.86[14]	22.93[2]	21.51	2.28	6[2]	260	Linear

Table 2. (continued)

Cluster	X-ray (H_o = 50)					Optical (H_o = 75)			Radio (H_o = 75)					
	L_x ergs/sec	$\dot{M}$ M_o/yr	t_{cool}/t_{Hubble}	R_{cool} (kpc)	P_c $\times10^{-11}$dyn cm^{-2}	z	σ_R km/sec	L_{line} ergs/sec	P_{20} (W/Hz)	P_6 (W/Hz)	α	LLS (kpc)	P_{min} $\times10^{-11}$	Morph.
A2107	43.85	--	1.9	--	2.0	0.0421	--	--	<21.79[2]	<20.89	--	--	--	--
A2124	43.75	--	2.0	--	0.9	0.0669	--	--	--	<21.17	--	--	--	--
A2199	44.32	119	0.2	166	3.5	0.0305	784	40.04[15]	24.81[7]	≈23.97	1.35	85	3[9]	Bipolar
A2244	44.83[1]	82	0.6	180	3.6	0.0997	--	--	--	<21.47	--	--	--	--
A2271	43.43	--	8.3	--	1.4	0.0616	--	--	--	<21.13	--	--	--	--
A2319	44.62	--	1.8	--	9.5	0.0529	--	<40.72[15]	<21.83[2]	<21.06	--	--	--	--
A2420		--	2.0	--	2.5	0.0838	--	--	--	22.86	--	13	0.8	WAT?
A2593	43.64	--	2.8	--	0.8	0.044	--	--	--	<20.85	--	--	--	--
A2626	43.93	35	0.8	119	1.6	0.0562	--	--	23.51[2]	22.68	1.37	23[2]	263	Bipolar
A2634	43.56	--	2.3	--	0.6	0.0322	927	<37.78[16]	25.19[10]	24.75[10]	0.7	390[11]	0.5[11]	WAT
A2670	44.00	--	2.0	--	2.8	0.0749	890	--	--	22.36†	--	--	--	Point

[1] From Arnaud (1989)
[2] O'Dea & Baum (1986)
[3] Fabian et al. (1985)
[4] Burns & Ulmer (1980)
[5] Slee & Reynolds (1984)
[6] Pedlar et al. (1988)
[7] Owen et al. (1982)
[8] Jaffee & Perola (1974)
[9] Burns et al. (1983)
[10] Kellermann et al. (1969)
[11] Eilek et al. (1984)
[12] Romanishim (1987)
[13] Hu et al. (1985)
[14] Heckman (1981)
[15] Cowie et al. (1983)
[16] O'Dea et al. (1986)

† Offset 8" South of measured position

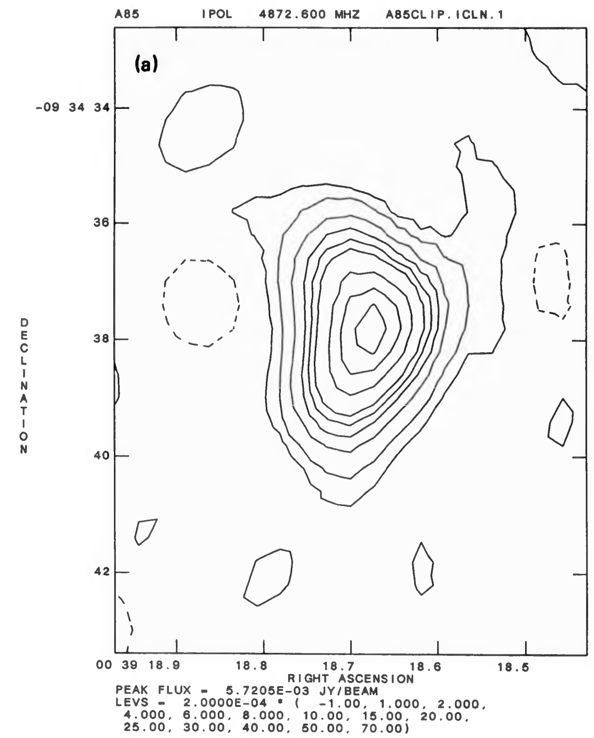

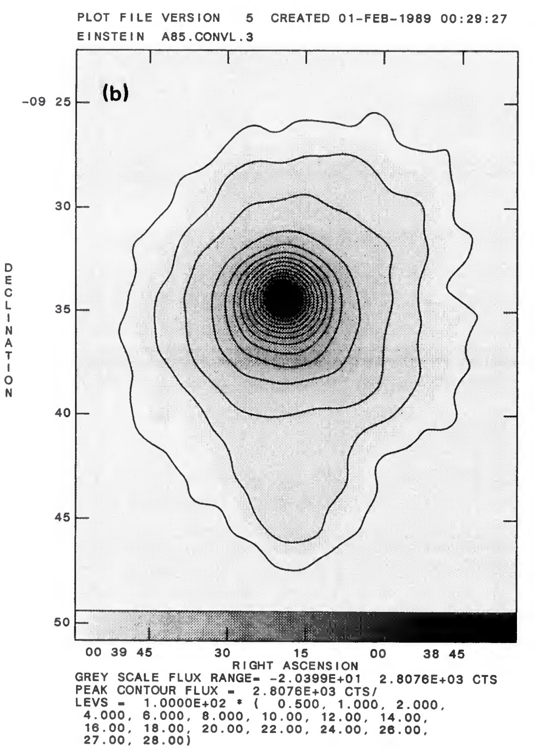

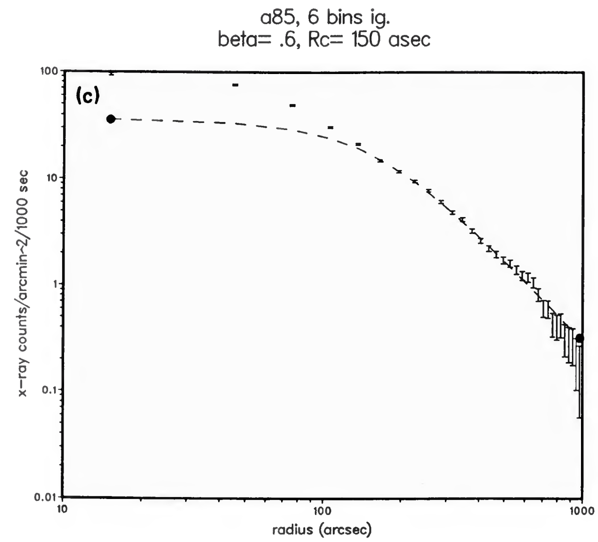

FIG. 1. Comparisons of the radio and x-ray data for clusters with resolved radio sources and cooling cores. **Abell 85.** Inner six bins were dropped for King model fit yielding a reduced χ^2 of 1.0 and $r_x = 150''$–$250''$, $\beta = 0.57$–0.65 (range is 90% confidence interval). (a) VLA image. (b) Smoothed *Einstein* map. (Note change in scale from VLA map.) (c) X-ray surface-brightness profile and the best-fit King model.

muthally binning the data in concentric rings about the centroid. The surface-brightness profile was then fit to the isothermal King (1962) approximation for a gas in hydrostatic equilibrium in the form

$$S(r) = S_0[1 + (r/r_x)^2]^{-3\beta + 1/2},$$

where r_x is the x-ray core radius and β is the ratio of the kinetic energy in the cluster galaxies to the thermal energy in the gas (see, e.g., Forman and Jones 1982). The fitting was performed in a fashion similar to that described in Jones and Forman (1984). A grid of two-dimensional King models with β ranging from 0.4 to 1.0 and r_x ranging from $20''$ to $1000''$, each convolved with 1.5 arcmin Gaussian beam, was generated. Surface-brightness profiles were constructed from the models. We then compared the observed cluster profile to the grid of models to determine which values of r_x and β produced the minimum in χ^2. Since there are sometimes central x-ray excesses above that extrapolated from the outer King model, we also varied the number of points included in the profile fit, dropping up to eight central points

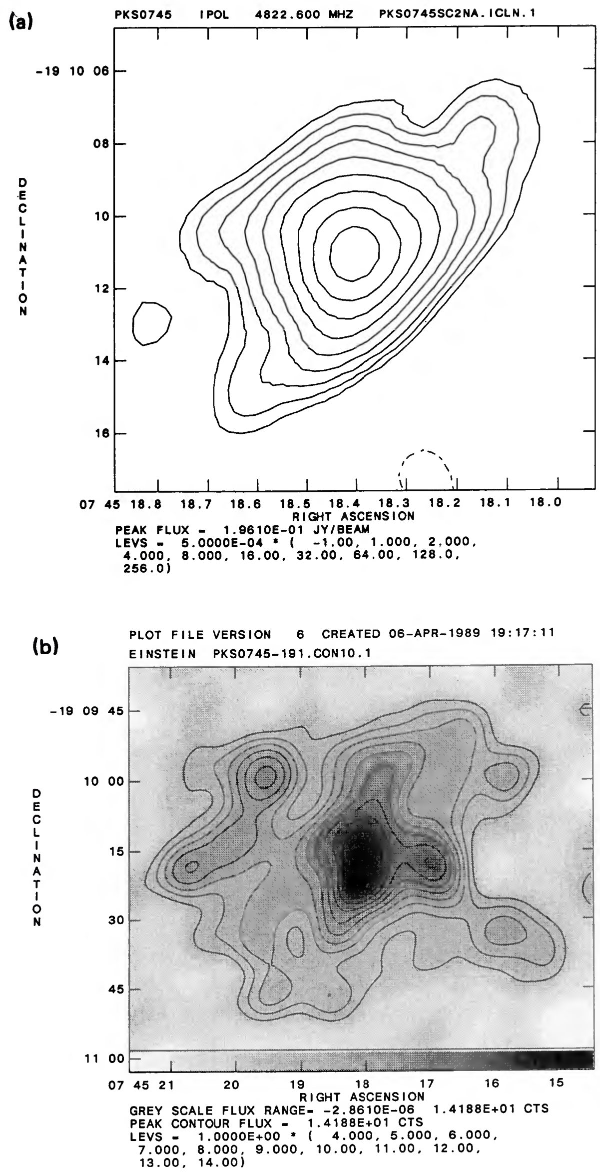

FIG. 2. Same as Fig. 1. (a), (b) **PKS 9745 − 191**. The x-ray image is from the Einstein HRI. The map was convolved with a circular Gaussian beam with FWHM 5 arcsec.

and fitting only the outer cluster. In cases with "cooling cores," the χ^2 value was reduced by fitting only the outer cluster. The results of our best fits are shown in Figs. 1–7, where the figures illustrate clusters with cooling cores, and Figs. 8 and 9 illustrate clusters with central cooling times greater than a Hubble time.

d) Comments on Individual cD Galaxies

Abell 85 (Fig. 1). The cD in this cluster has a similar amorphous radio morphology, size, and steep radio spectrum to that in 0745 − 191 described below. However, it is considerably less luminous at radio frequencies. There is good agreement between the $\dot{M}$ determined by Arnaud from the *Einstein* IPC (as illustrated by the x-ray excess in Fig. 1 and that determined from the spectral lines of the *Einstein* SSS (Mushotzky and Szymkowiak 1988). Heckman (1981), Cowie *et al.* (1983), and Hu *et al.* (1985) have each detected optical emission lines associated with the core region of the cD. The optical emission is relatively compact with slight extension on a scale of 10″–15″. Thus, the radio and emission-line structure appear to be cospatial.

PKS 0745 − 191 (Fig. 2). This is the only cluster in our sample that is not in the Abell catalog. However, its properties are exceptional in many ways. The cluster surrounding 0745 − 191 has the highest x-ray luminosity of any cluster in our sample (e.g., Arnaud *et al.* 1987). It has strongly centrally peaked x-ray emission leading Fabian *et al.* (1985) to suggest that its mass accretion rate $\dot{M}$ may be as high as 1000 $M_\odot$/yr (Arnaud, however, has revised this downward as in Table II.) The radio power of this source is also the highest in our sample and the radio spectrum is relatively steep (Hunstead *et al.* 1978). The radio morphology is best described as amorphous (see Sec. III) as can be seen in Fig. 2 with prominent "wings" at position angles of about + 45° and − 45°. This structure is also seen in 20 cm VLA maps by Fabian *et al.* (1985) and Baum *et al.* (1988). Romanishin (1987) has found an extensive system of bright Hα filaments that is comparable in luminosity to that in NGC 1275 in the Perseus cluster (once thought to be uniquely "Hα overluminous"). Baum *et al.* (1988) find that the Hα + [N II] emission is resolved and roughly cospatial with the radio emission.

Abell 133. The central cD was not detected by our survey at this resolution and sensitivity. However, Slee and Reynolds (1984) did detect and map the remarkably steep spectrum ($\alpha \approx 2.8$), amorphous emission at 6 and 20 cm using the VLA in its smaller (C and D) configurations. The combination of high resolution and steep spectral index apparently did not allow us to detect any of the resolved, steep-spectrum emission from this source. Joshi *et al.* (1986) also mapped A133 with the Ooty Synthesis Radio Telescope at 327 MHz. Hu *et al.* detected faint Hα + [N II] emission confined to within a few arcseconds of the galaxy core.

Abell 401. This cluster was previously mapped using the VLA by Burns and Ulmer (1980). Although there are several tailed sources in the cluster, the cD is radio quiet. No optical emission lines have been detected for the central cD.

Abell 496. The radio emission associated with the cD galaxy is the only real flat-spectrum radio source in Table I. It is marginally resolved with a deconvolved FWHM of 0.3″. This small size combined with the flat spectrum suggests that we are seeing emission only from the very core of the galaxy near the central engine. Hu *et al.* (1985) find a somewhat extended optical emission-line region that is about 8″ in size. However, they find no evidence for filamentation as originally claimed by Fabian *et al.* (1981).

Abell 1795 (4C 42.26) (Fig. 3). The relatively strong (0.25 Jy), but small diameter radio source associated with the cD has an extended tail-like morphology. The strong core (55 mJy) was used to self-calibrate the visibilities and thus improve the dynamic range of the low-surface-brightness extended structure. The higher-resolution 6 cm map in van Bruegel *et al.* (1984) reveals two very small jets with lengths < 1 kpc. They appear to feed into the two tails at nearly right angles. This radio source also appears to have a very high-rotation measure (F. N. Owen, private communication), not unlike that seen in other radio galaxies (e.g., M87) in cooling cores. Cowie *et al.* (1983), van Bruegel *et al.* (1984), and Johnstone and Fabian (1988) each noted optical emission-line structure in the radio galaxy that extends out to a radius of about 50 kpc, the largest extent of any cD in this sample. van Breugel *et al.* and Baum and Heck-

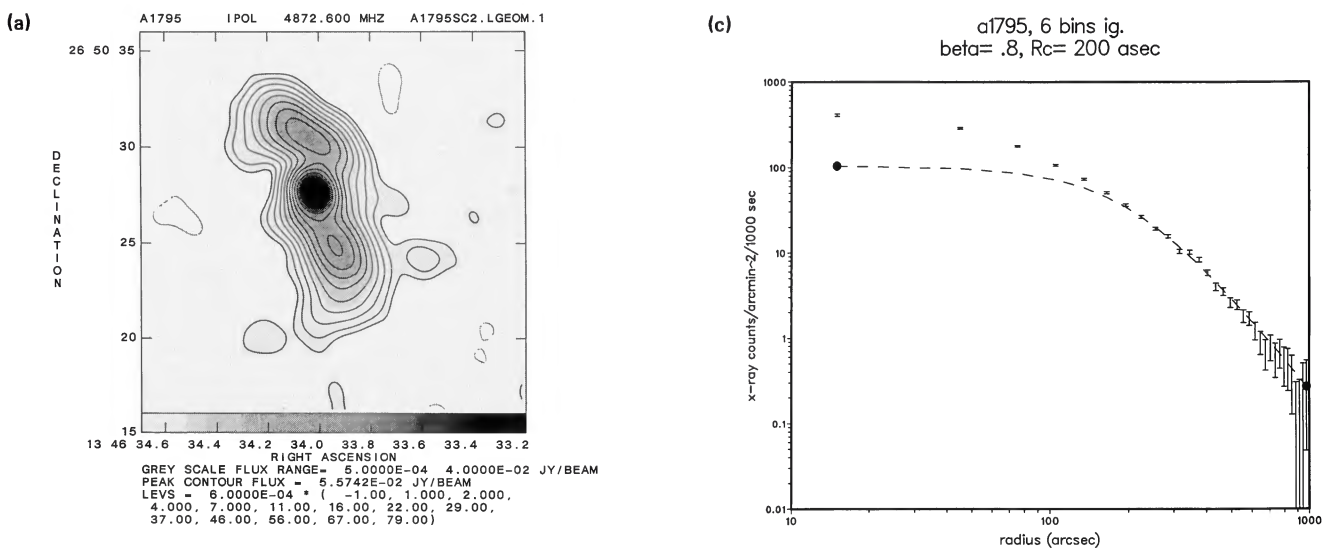

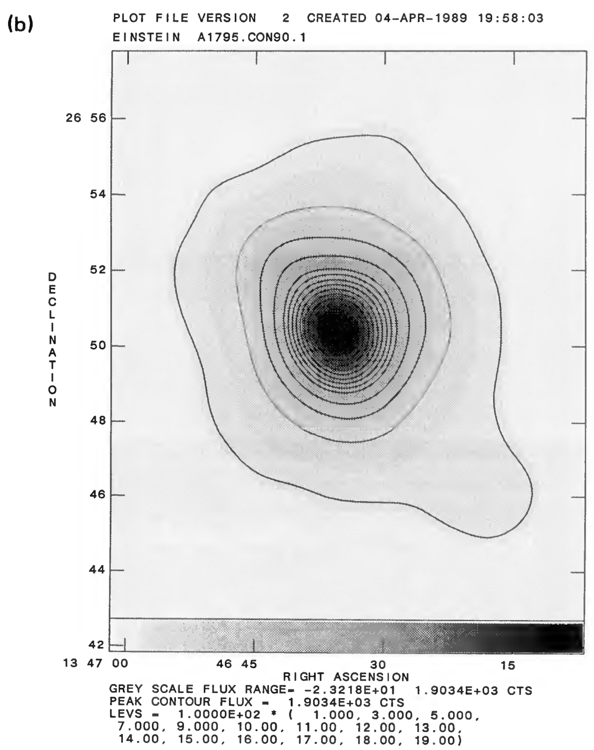

FIG. 3. Same as Figs. 1(a)–1(c). **A1795**. Inner six bins were dropped for King model fit yielding a reduced $\chi^2 = 1.1$, $r_x = 175''$–$300''$, and $\beta = 0.75$–1.0.

man (1986) also noted a strong positional coincidence between the inner emission line filament system and the radio source.

Abell 2029 (Fig. 4). We describe the source morphology as dual jet. This is only one of about four sources in this sample that displays well-defined jet structure, a surprisingly low percentage. Recently, Sumi *et al.* (1989) mapped the source at higher resolution revealing a series of bends and knots in the jet structure. They suggest that the small size and morphology of this source are due to interaction of the jet plasma with a "pressure wall" in a possibly supersonic cooling inflow. Hu *et al.* do not detect any emission-line gas associated with the cD.

Abell 2052 (3C 317) (Fig. 5). This is the closest of the class of radio source that we define as amorphous. Thus, it is the brightest and best resolved. One scan of A-array data was added to the B-array visibilities in the map in Fig. 5. The source was self-calibrated. A natural weighting taper was applied to the visibilities to better emphasize the extended halo around the unresolved core. This core-halo structure appears to be prototypical of many of the steep spectrum, small radio sources often associated with central galaxies in cooling core clusters. It also has a high rotation measure (F. N. Owen, private communication). Baum *et al.* (1988) found several bent, emission-line filaments that are cospatial with the radio emission. They suggest a possible connection between the radio plasma and the optical filaments. There is also a substantial central x-ray excess as seen in Fig. 5.

Abell 2063 (Fig. 6). The map in Fig. 6 reveals a source structure that is composed of an unresolved core with a pos-

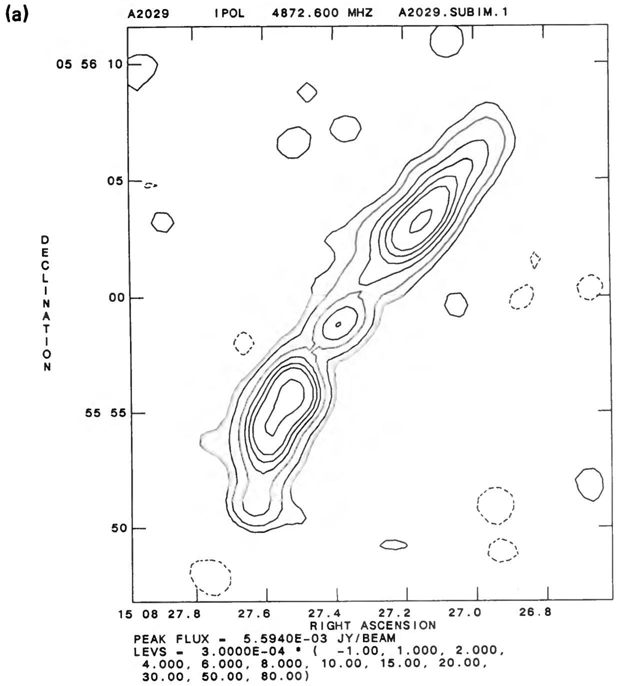

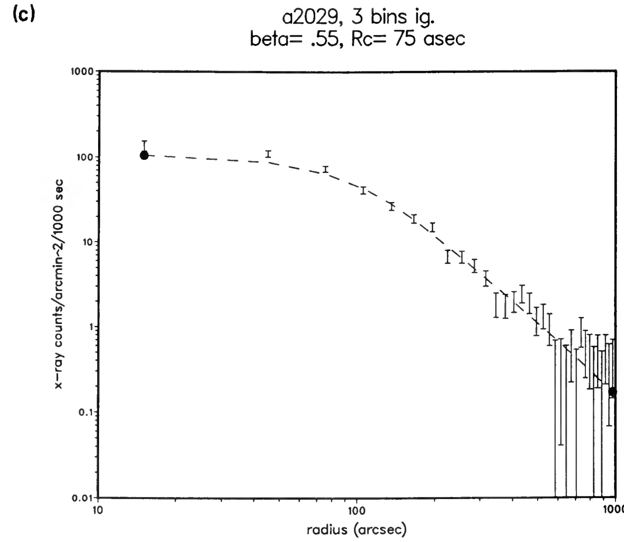

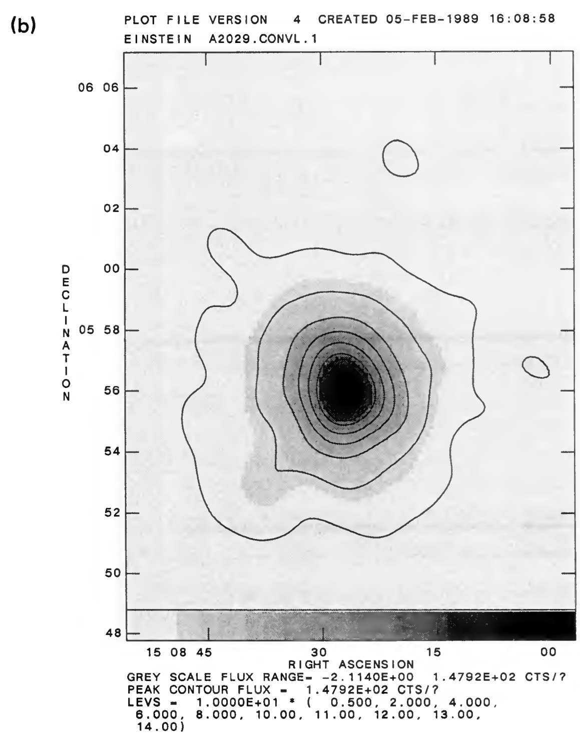

FIG. 4. Same as Figs. 1(a)–1(c) **A2029**. Inner three bins were dropped for King model fit. $\chi^2 = 0.8$, $r_x = 25''$–$88''$, and $\beta = 0.53$–0.65.

sible extension to the west. At 20 cm, O'Dea and Baum (1986) detect and map this linear extension. Our 6 cm data and the O'Dea and Baum 20 cm data suggest that the structure has a very steep spectral index (2.3). Heckman (1981) does not find any emission-line gas associated with the cD.

Abell 2199 (3C 338) (Fig. 7). Burns *et al.* (1983) have previously published the most detailed radio data on this source. We have taken these 6 cm VLA data and reprocessed the maps using the self-calibration algorithms now available in AIPS. A substantial improvement in the dynamic range resulted in the map shown in Fig. 7. Again, natural weighting was used to better emphasize the extended lobes. As noted by Burns *et al.*, this radio source is basically bipolar with no well-defined jets emanating from the compact core (associated with the brightest of four nuclei). There is, however, a peculiar steep-spectrum ridge that lies about 10″ south of the core and runs along an east–west direction. Cowie *et al.* (1983) found emission-line gas associated with the brightest (radio-loud) nucleus, but no extended emission or filaments. A cooling core appears present from the fit to the x-ray surface-brightness profile and the short cooling time.

Abell 2420 (Fig. 8). The map in Fig. 8 suggests that the

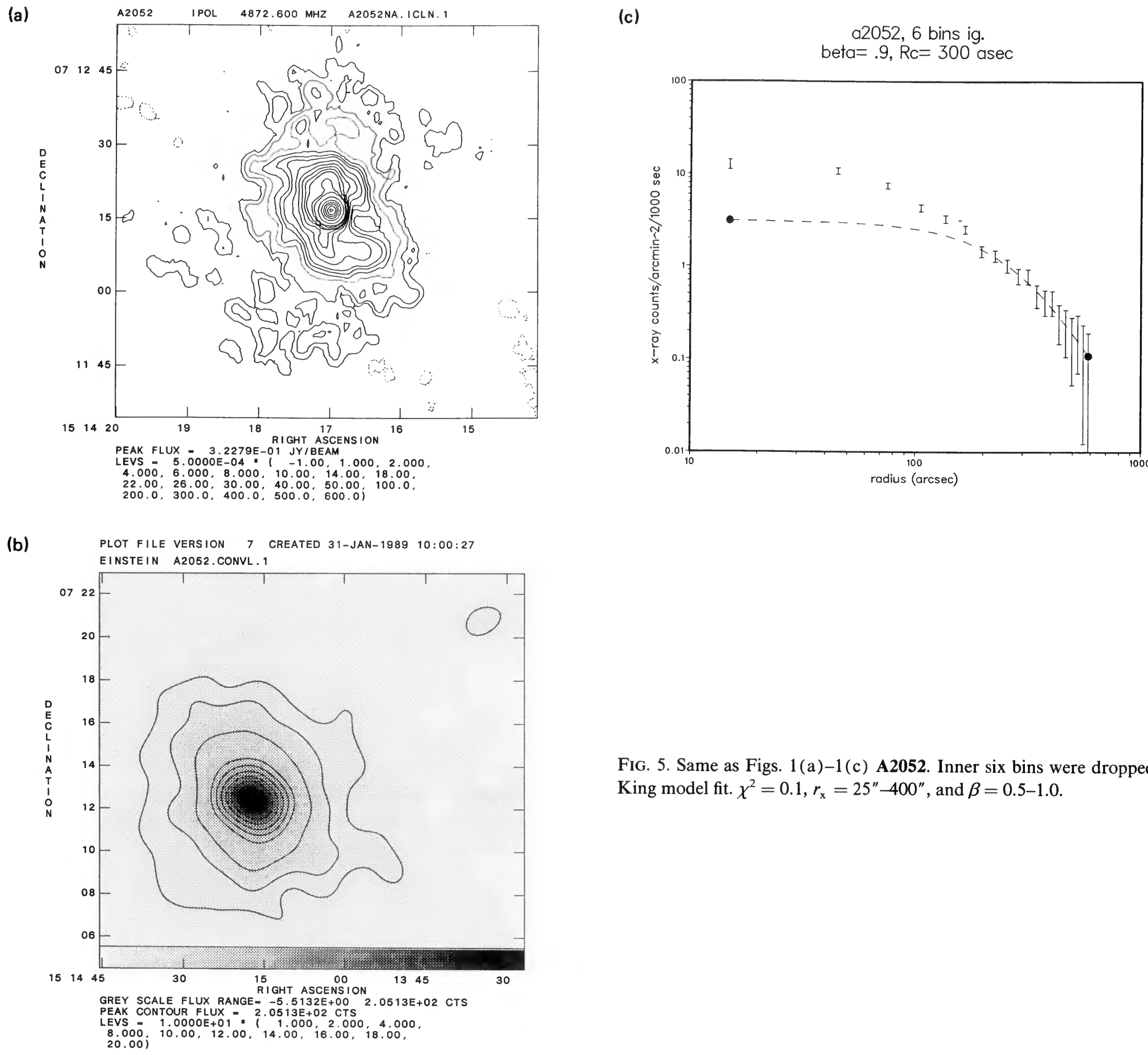

FIG. 5. Same as Figs. 1(a)–1(c) **A2052**. Inner six bins were dropped for King model fit. $\chi^2 = 0.1$, $r_x = 25''$–$400''$, and $\beta = 0.5$–1.0.

source is a relatively low-luminosity WAT. The centroid of the cD is coincident with the brightest, easternmost of the radio components. Although there may be a slight excess of x-ray emission near the core, the cooling time is greater than the Hubble time, thus indicating that the cluster does not have a cooling core.

Abell 2626 (4C 20.57). The 6 cm radio emission consists of a single, unresolved component with flux density 7.5 mJy, coincident with the optical galaxy measured position. O'Dea and Baum (1986) report the detection of extended emission with a diameter of about 20 kpc at 20 cm. The resulting spectral index is > 1.4. Similarly, Roland *et al.* (1985) observed extended bipolar structure at 49 and 20 cm using the Westerbork array; the apparent spectral index is $\lesssim 2.2$. Therefore, this is apparently another example of a small, amorphous, steep-spectrum source in a cooling flow.

Abell 2634 (3C 465) (Fig. 9). This cluster source is the prototypical example of a WAT. The radio map in Fig. 9 illustrates only the central region of a much more extended tailed source. This map is from Eilek *et al.* (1984) with a resolution of 0."8 to 0."5 (P.A. = 37°), somewhat higher than other maps in this survey. The x-ray surface brightness has a central excess, but the core cooling time is greater than a Hubble time (Table II). The *Einstein* HRI image of A2634 (not shown) reveals a marginally resolved (nonthermal?) source at the core that may be the origin of the excess. We conclude, along with Arnaud (1989) and Jones and Forman (1984), that A2634 does not have a cooling core. There is an interesting diffuse x-ray component in Fig. 9(b) to the northwest of the cD galaxy that does not have an optical ID according to Eilek *et al.* (1984). This was removed in the King model fit to the x-ray surface brightness in Fig. 9(c). 3C 465 is the largest radio source in our sample, has one of the flattest integrated spectra, and the cluster does not have a cooling core or any optical emission-line filaments (O'Dea *et al.* 1986).

e) Summary of X-Ray, Optical, and Radio Properties

A summary of the multifrequency properties of the cD galaxies and their surrounding clusters is given in Table II.

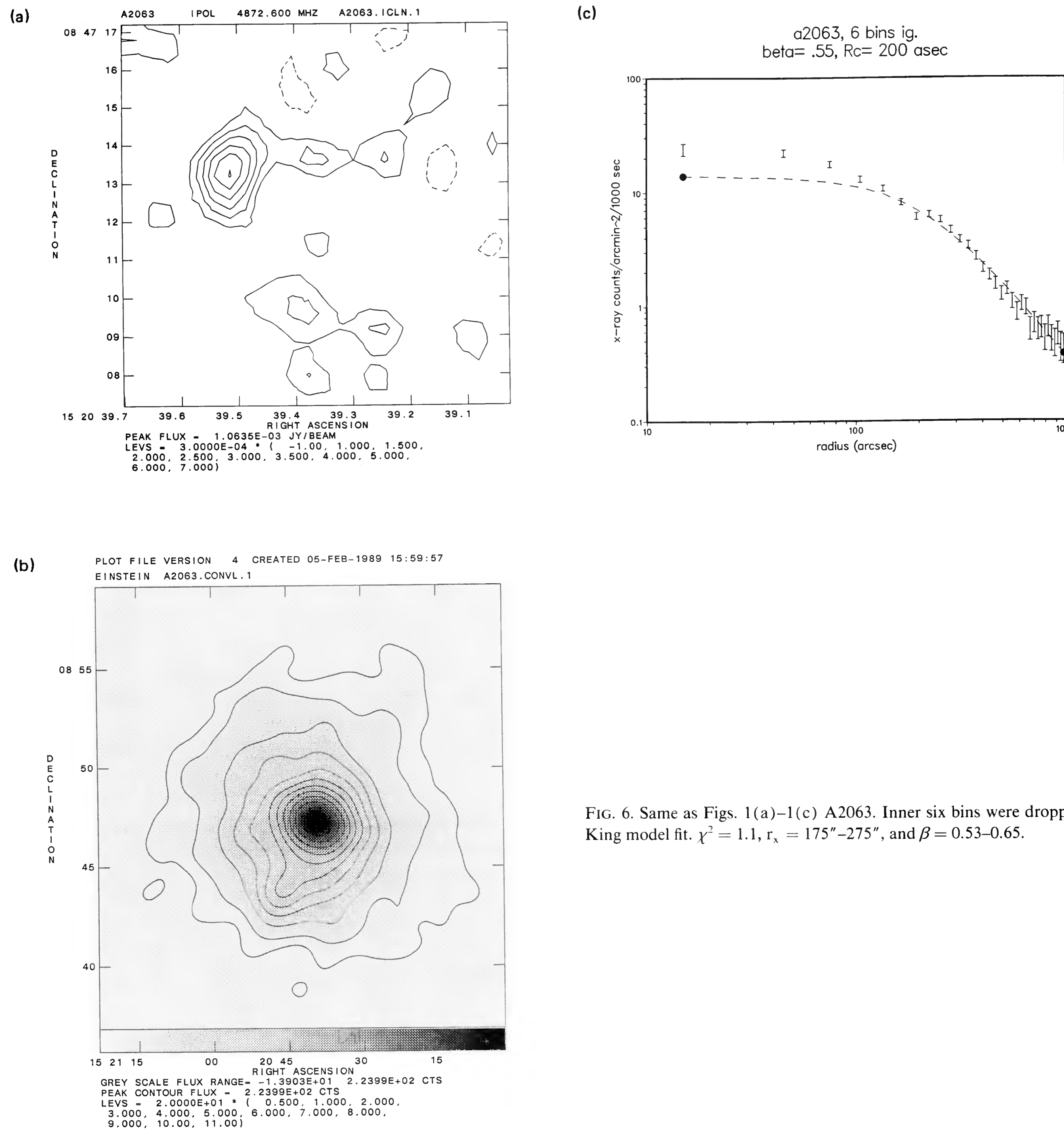

FIG. 6. Same as Figs. 1(a)–1(c) A2063. Inner six bins were dropped for King model fit. $\chi^2 = 1.1$, $r_x = 175''$–$275''$, and $\beta = 0.53$–0.65.

References to quantities not derived in the present work are noted in superscripts. The table is divided into three parts according to frequency. Part I contains the x-ray data (mostly derived from Arnaud 1989) as follows:

Column 1. Total x-ray luminosity in the 0.5–3.0 keV band from the *Einstein* observations reported by Jones and Forman (1984) and Abramopoulous and Ku (1983).

Column 2. Estimated cooling flow accretion rate.

Column 3. Ratio of the x-ray gas cooling time to the Hubble time.

Column 4. Radius within which the cooling time is less than the Hubble time.

Column 5. Central pressure determined from deconvolved densities and temperatures as described by Arnaud (1988). All x-ray quantities have been left in units of $H_0 = 50$ km/s/Mpc to maintain the original accuracy of derived values. The optical and radio parameters are expressed in units of $H_0 = 75$ km/s/Mpc and $q_0 = 0$. Since only relative comparisons are made between the x-ray, and the radio and optical in what follows, we do not intermix the units.

Part II of the table contains optical data as follows:

Column 6. Measured redshift as listed in Struble and Rood (1987).

Column 7. Cluster radial-velocity dispersion as listed in Stuble and Rood (1987).

Column 8. Luminosity of Hα line emission near the cD. Values are estimated from Heckman *et al.* (1989) with original references noted as superscripts.

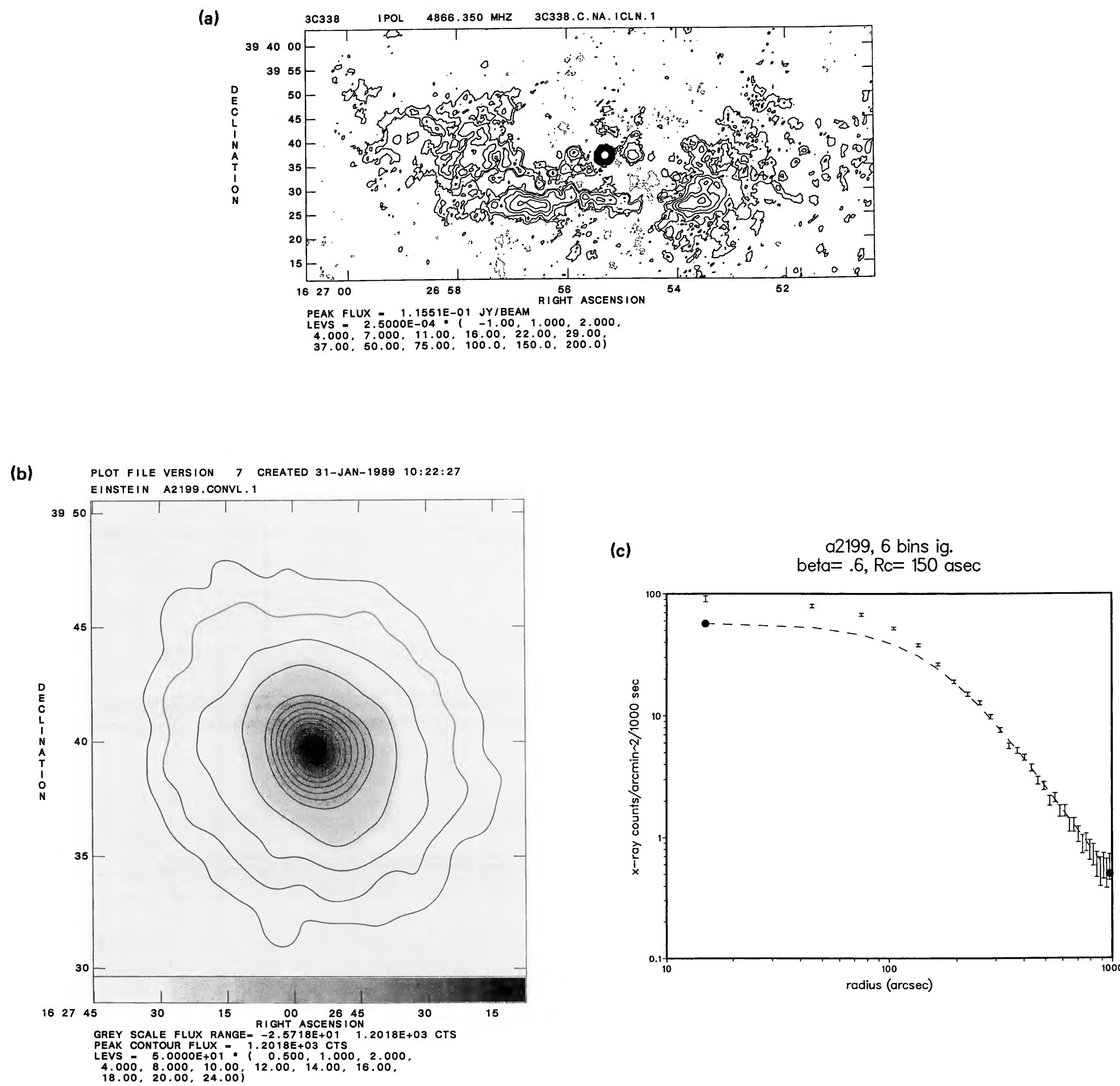

FIG. 7. Same as Figs. 1(a)–1(c) A2199. Inner six bins were dropped, $\chi^2 = 0.7$, $r_x = 150''$–$250''$, and $\beta = 0.57$–0.65.

Part III of the table contains radio data as follows:

Column 9. Integrated radio power at 20 cm.

Column 10. Integrated radio power at 6 cm. Flux densities were converted into powers using the formula (e.g., von Hoerner 1974):

$$P_6 = 1.91 \times 10^{24} S_6(\mathrm{mJy}) z^2 (1+z)^{3+\alpha} \times (1+z/2)^2/(1+z)^4 \ \mathrm{W/Hz},$$

where α is the spectral index as defined below.

Column 11. Spectral index defined by $S_\nu \propto \nu^{-\alpha}$.

Column 12. Largest linear size (LLS) determined from the angular diameter θ according to (e.g., von Hoerner 1974):

$$\mathrm{LLS} = 19.39\theta z(1+z/2)/(1+z)^2 \ \mathrm{kpc}.$$

Column 13. Minimum pressure of extended radio components derived following the prescription in Burns *et al.* (1979).

Column 14. Radio morphology.

III. RELATIONSHIP BETWEEN RADIO, X-RAY, AND OPTICAL EMISSIONS

Valentijn and Bijleveld (1983) and Jones and Forman (1984) previously suggested that there is a direct relationship between the levels of x-ray and radio emission associated with centrally dominant galaxies in rich clusters. However, Owen *et al.* (1984) and Zhao *et al.* (1989) cautioned that the relationship may be more complex. The current

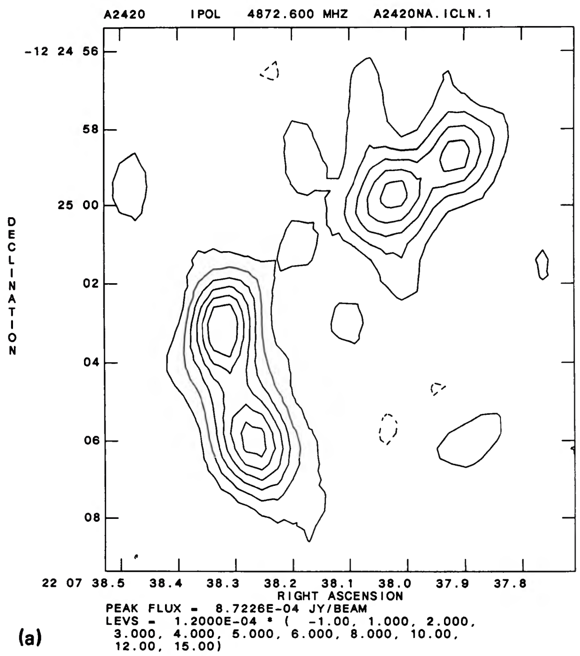

(a)

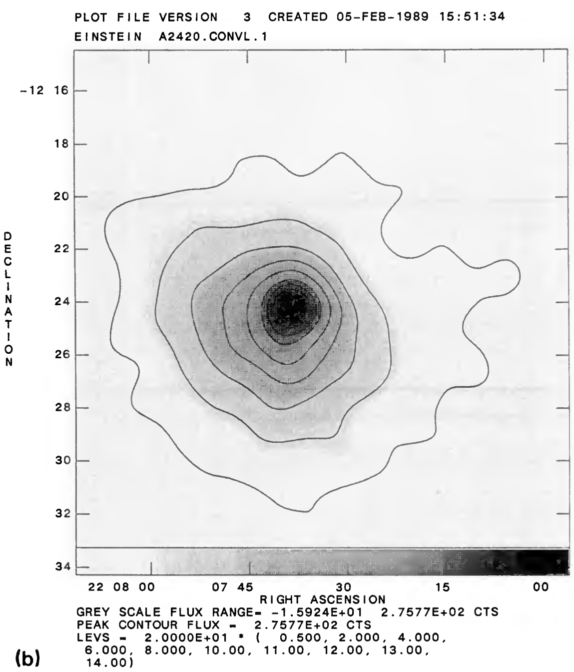

(b)

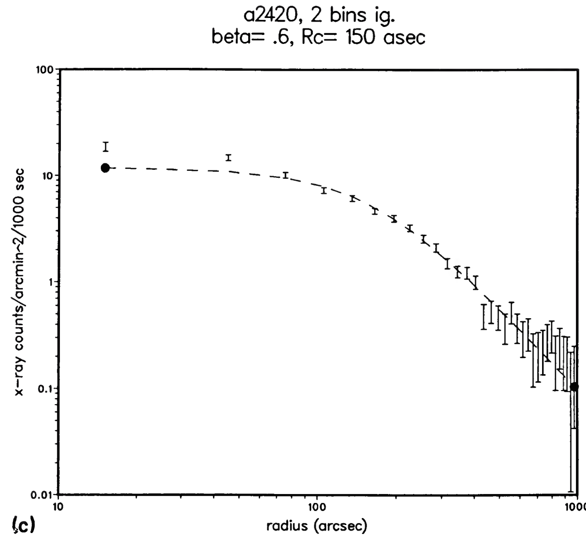

(c)

FIG. 8. Same as Fig. 1 except clusters without cooling cores and with extended radio sources are displayed. (a)–(c) **A2420**. Inner two bins were dropped for King model fit. $\chi^2 = 0.6$. $r_x = 25''–175''$, and $\beta = 0.47–0.65$.

sample allows us to examine this question for cD galaxies using better radio and x-ray data than previously available.

a) Radio Power and Accretion

Valentijn (1988) has recently suggested that a strong correlation exists between radio power and x-ray luminosity for dominant cluster galaxies. He interprets this correlation as due to the direct fueling of the radio engine by accretion of cooling gas onto the central galaxy. For our sample in Table II, we do *not* find any such correlation between L_x and P_6. For a given x-ray luminosity, there is a wide range of radio powers. For example, between $44.5 < \log(L_x) < 45$, the 6 cm radio powers range from $\lesssim 21$ to ≈ 24.3. Zhao *et al.* (1989) similarly did not find any correlation for nearby Abell clusters with central dominant galaxies at 20 cm. The integrated L_x may not be a good measure of cooling accretion that takes place only in the central region of a cluster. In addition, the lack of a statistically defined sample in the x-ray is a concern.

There does appear to be a trend, seen both in Table II and in Fig. 10, suggesting that clusters with central cooling cores are more likely to be radio sources than cDs without such cores. Seventy-one percent (10/14) of cDs with cooling cores have radio emission with flux densities $\gtrsim 0.2$ mJy. However, only 23% (3/13) of cDs without cooling cores have detected radio emission at this level. Applying a contingency table test (Lindgren 1962) to these detection statistics, we find that the null hypothesis of independence between a cooling core and radio emission is rejected at the 98.5% level. A similar significance test using survival analy-

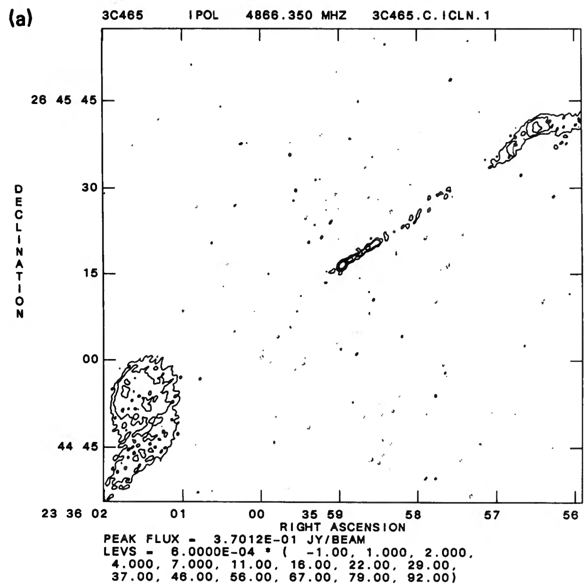

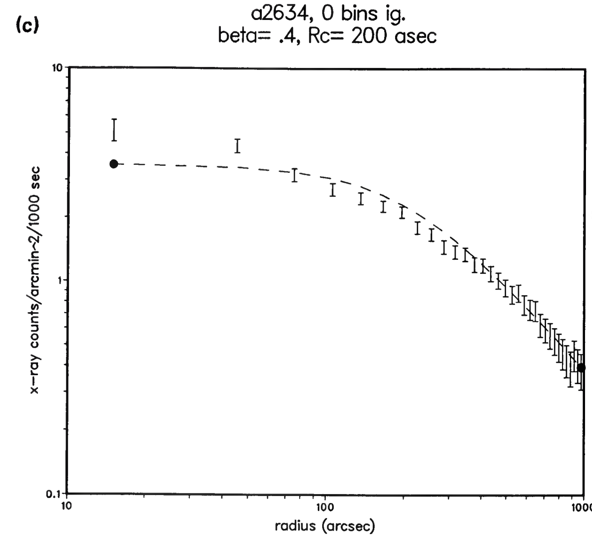

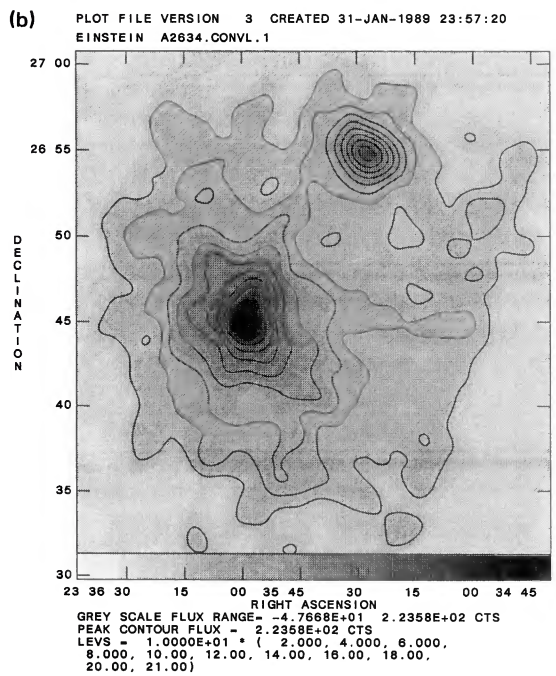

FIG. 9. Same as Figs. 8(a)–8(c) **A2634**. No bins were dropped for King model fit. $\chi^2 = 1.7$, $r_x = 175''–575''$, and $\beta = 0.35–0.65$.

sis (Feigelson and Nelson 1985) suggests that the null hypothesis is rejected at the 98%–99% confidence level. Although the fraction of noncooling cores with radio emission is smaller, it is still significant, suggesting that mechanisms other than infall of ICM gas can generate a radio source.

In Fig. 10, we have plotted central accretion rates, $\dot{M}$, versus radio power at 6 cm. This plot is complementary to that in O'Dea and Baum (1986) since $\dot{M}$ is derived from the central x-ray excess. Clusters with large central accretion rates, such as PKS 0745 − 191, tend to be powerful sources of compact radio emission. However, there are exceptions. The most notable is A644 which has a purported cooling flow with $\dot{M} = 326\ M_\odot/\mathrm{yr}$, but yet it is radio quiet.

On the other hand, it appears that clusters without a cooling core are often radio quiet. There is a substantial collection of clusters in the lower left portion of Fig. 10 that have small or absent accretion and no detectable radio emission. However, WAT sources such as 3C 465 are notable exceptions in that these radio sources are very luminous (comparable to the brightest sources found in cooling cores) and exist within clusters without x-ray cooling cores. These exceptions may suggest that the mechanisms responsible for generating and shaping the radio emission are more complex than the simple accretion fueling arguments that were previously advocated (e.g., Valentijn 1988).

This comparison between the x-ray and radio emissions is fundamentally limited by the quality and quantity of the currently available x-ray data. The lack of a complete sample coupled with the poor angular resolution (1.5 arcmin) of the x-ray sample restricts our ability to interpret any relation-

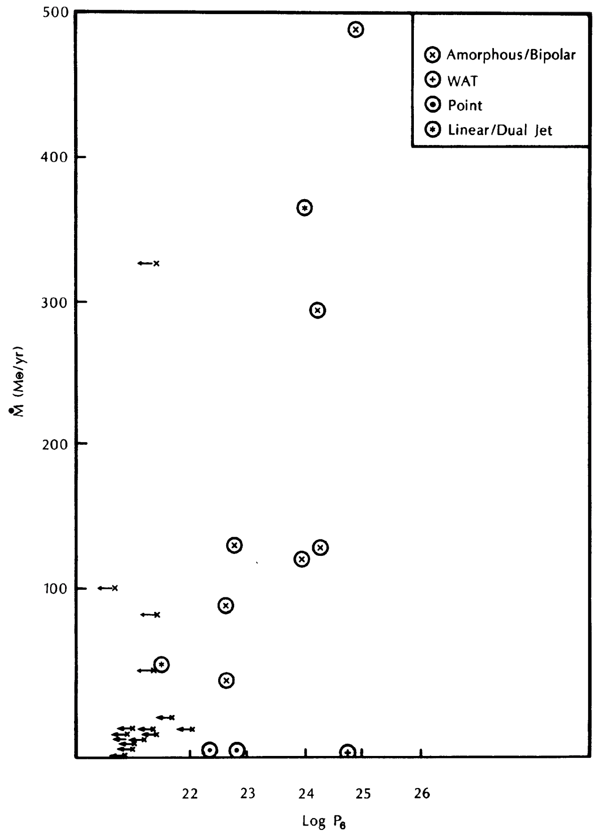

FIG. 10. Radio power at 6 cm versus accretion rate (Ṁ) derived from x-ray deconvolutions by Arnaud (1988). Symbols indicate different radio-source morphologies.

ships. In particular, it is difficult to decouple the general cluster gas from that purportedly falling onto the cluster core via cooling. Ṁ, for example, may decline with decreasing distance from the core as mass drops out of the flow (e.g., Fabian 1988). The central Ṁ is the most relevant quantity to compare with P_6. However, only an effective global average of Ṁ is available with current data. Furthermore, only a small fraction of the global Ṁ is needed to produce the observed radio power for conversion efficiencies, ϵ, of $\sim 1\%$ ($L_{\rm radio} = \epsilon \dot{M}_c c^2$, where $\dot{M}_c$ is the accretion rate onto a central blackhole).

b) Radio Morphologies

In addition to the differences in probability of radio emission, there also appear to be fundamental differences in radio structure between sources in clusters with and without cooling cores. Owen, Burns, and White (1984) first noted that wide-angle-tailed (WAT) sources occur almost exclusively in clusters without cooling cores. The prototypical example is 3C 465 in A2634. WATs are often characterized by a large linear size ($\gtrsim 100$ kpc, well outside the optical extent of the galaxy), "normal" integrated radio spectral index (0.7), extended jets (10–20 kpc) emanating from the galaxy nucleus, and bent and edge-darkened radio tails. Two of the three sources in Table II associated with noncooling cores are WATs.

There appears to be some interesting diversity in source structure for radio galaxies in cooling cores. Most of the sources are extended, but all are much smaller in linear diameter than 3C 465. This is discussed further below. Several of the cluster sources (A1795, A2029, A2063) have jetlike structure. Some, such as 3C 338 in A2199 do not have detectable jets. What is most interesting, however, are two features that are common to most of the cooling core radio galaxies. First, nearly all the radio sources in cooling cores have steep radio spectra ($\alpha > 1$), with some such as A133 and A2063 being extraordinarily steep ($\alpha > 2$). Second, most of the sources have either poorly collimated, roughly bipolar structures (e.g., A1795, A2199) or amorphous core-halo morphologies (e.g., A2052). This outer amorphous, diffuse radio emission is seen in other clusters with cooling cores such as in Perseus (3C 84; Pedlar *et al.* 1988) and Virgo (M87; Feigelson *et al.* 1987). There appears to be an interesting class or component of radio galaxies, which is best termed amorphous, that is often associated with cooling cores.

c) Radio-Source Sizes

There are two factors that likely control the size of a radio source. The first is the momentum or kinetic energy of the outflowing plasma. If the extended radio emission is ultimately derived from conversion of kinetic energy, as suggested by most *in situ* particle acceleration models (e.g., Eilek 1982), then the radio power per unit length should be a rough measure of the kinetic energy in the plasma outflow. The second factor is the dynamic or thermal pressure of the surrounding medium (i.e., confinement). For plasma flows that are moving subsonically with respect to the ambient medium (probably true for relaxed or diffuse structures), then the external pressure will be dominated by the thermal pressure.

In Fig. 11, the thermal pressures at the centers of the clusters computed from the x-ray parameters are plotted against radio power for the radio-loud cDs in this sample. The sources are further distinguished by source size. It would appear that both factors noted above influence the intrinsic source size to differing degrees. For example, one of the smallest sources in the sample, PKS 0745 − 191, is also in the cluster with the highest external pressure. Similarly, the largest source in the sample, 3C 465 (which is also one of the most powerful), is in the cluster with the lowest external pressure. Most of the sources are intermediate in terms of pressure, radio power, and source size.

d) Optical Filamentation

There has been some debate concerning the origin of optical filamentation discovered in association with galaxies at the cores of cluster cooling flows. Fabian and colleagues (see, e.g., Fabian 1988) believe that the emission-line filament systems observed in galaxies such as NGC 1275 are due to thermal instabilities in the cooling accretion flow. They note that the timescales and spatial extents of the optical filaments are consistent with such instabilities within regions where the cooling times are less than a Hubble time. One might, then, expect a relationship to exist between the average rate of accretion and the integrated luminosity in the Hα line in cooling flow clusters. From Table II, 70% (7/10) of cDs with cooling cores have optical emission-line filaments (in clusters where narrowband optical imaging has been performed). We have plotted Ṁ versus $L_{\rm line}$ in Fig. 12

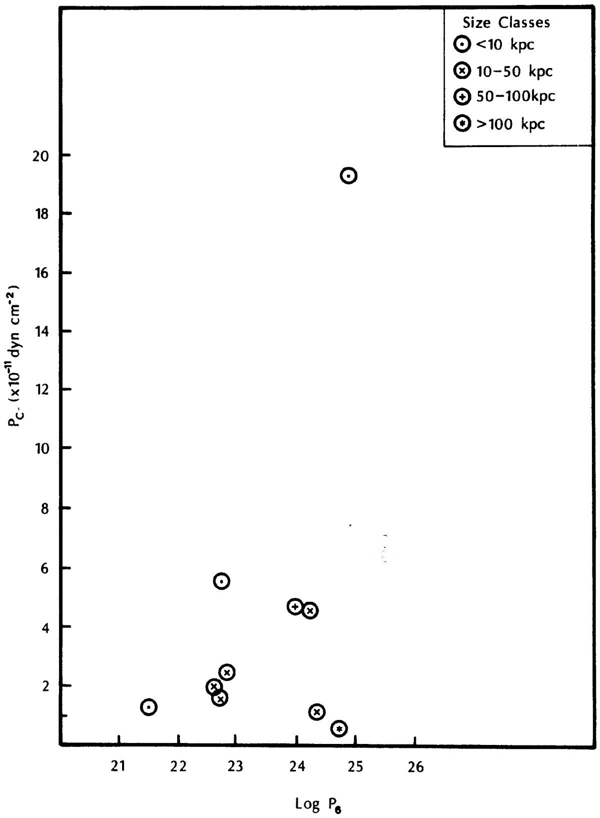

FIG. 11. Radio power at 6 cm versus thermal pressure (nkT) of the ICM derived from deconvolutions of the x-ray surface-brightness profiles. Symbols indicate different source sizes.

for clusters in our sample that have line measurements published in the literature as noted in Table II. Once again, the extraordinary cluster PKS 0745 − 191 has both the highest accretion rate and largest line luminosity. On the opposite end of this plot, there are several galaxies (e.g., A644) with no detected emission lines and very little or no accretion. In between, there is considerable scatter. At best, there is a weak relationship between accretion and optical filamentation as noted recently by Heckman *et al.* (1989).

Heckman and colleagues (see, e.g., Heckman *et al.* 1988, 1989; Baum and Heckman 1989a,b) and Pedlar *et al.* (1988) have suggested an alternative explanation for the filamentation. They note that many radio galaxies now have detected emission-line clouds coincident with the edges of radio features (hotspots or lobes). They suggest that since many of the purported cooling flow clusters are also sources of radio emission, then the filaments might have similar origins related to the interaction of the outflowing radio plasma with the gaseous environment. As noted in Sec. II, the optical emission-line filaments in the sample studied here are roughly cospatial with the radio emission. If this idea is correct, then one might expect to see a relationship between optical line emission and radio power (used again as a measure of momentum flux in the radio plasma). Again from Table II, 70% (7/10) of cDs with radio emission also have optical emission-line filaments. In Fig. 12, we have plotted radio power versus line luminosity. As in Fig. 12(a), there is a tendency for powerful radio sources (e.g., PKS 0745 − 191) to have strong line systems and weak or nonexistent sources (e.g., A401) to have little or no line emission. Once again, however, there is considerable scatter. In particular, two sources with clearly defined jets (in A2634 and A2029) have high radio powers but no detectable extended emission lines. There may be a correlation between $L_{\rm line}$ and P_6 for the amorphous/bipolar sources, but the sample is small. Hu *et al.* (1985) came to similar conclusions for their sample of dominant galaxies.

It is difficult to determine with this small sample which, if either, of the above is the intrinsic correlation. Heckman *et al.* (1989) have noted, for example, that at a given radio power, cooling core radio galaxies have an Hα luminosity that is typically 20 times greater than for radio galaxies that are not in cooling flows (also generally not in rich clusters). All three variables (i.e., Hα emission, cooling cores, and radio emission) may be related. The accretion could give rise to both the radio source and optical filaments. Alternatively, the radio emission may deposit energy into the surrounding gas producing excess x-ray emission (and the appearance of a cooling flow; see below) and, via compression, the optical filaments.

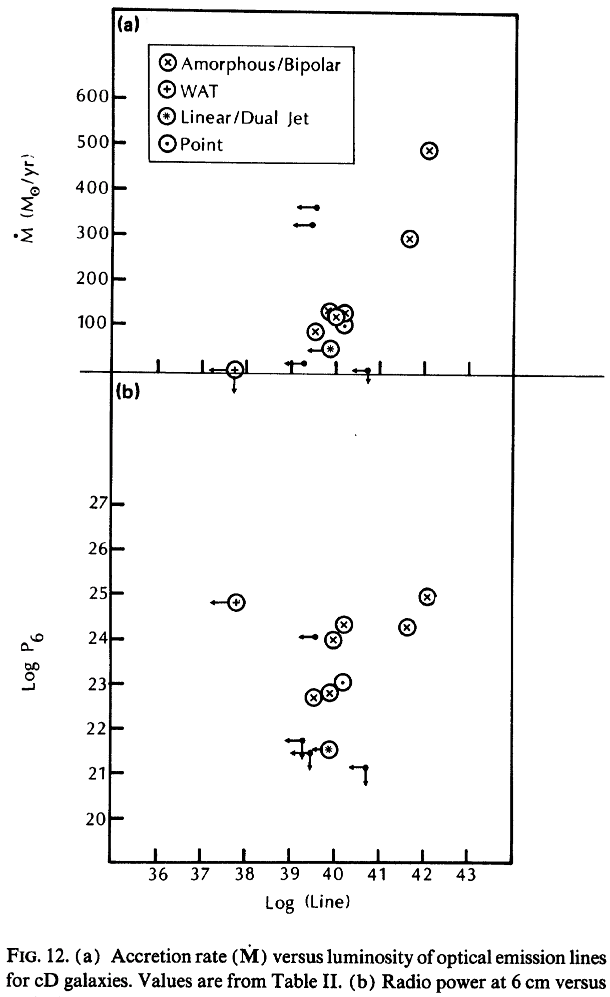

FIG. 12. (a) Accretion rate ($\dot{M}$) versus luminosity of optical emission lines for cD galaxies. Values are from Table II. (b) Radio power at 6 cm versus optical emission-line luminosity.

IV. DISCUSSION

There appears to be a strong coupling between cooling cores, as defined by central cooling times less than the Hubble time, and radio emission associated with the central cD galaxy in a cluster. We find that $> 70\%$ of cD clusters with cooling cores have central radio emission above 0.2 mJy at 6 cm. However, $< 25\%$ of clusters without cooling cores are radio loud. This disparity is striking and must point to an intimate connection between the processes giving rise to the radio and the x-ray emissions. The most obvious interpretation is that some of the cooling gas falls onto a central engine and fuels the radio source. The problem, as also pointed out recently by Zhao *et al.* (1989), is that only a very tiny fraction of the purported infalling gas ($< 10^{-6}$) is needed to fuel the radio source for reasonable conversion efficiencies between gravitational potential energy and synchrotron emission. There is an embarrassment of riches here in which the vast majority of the gas must never reach the core. Various mechanisms have been proposed to hide the infalling gas (e.g., formation of low-mass stars; see, e.g., Sarazin 1986), but none are totally convincing. If all the gas did fall onto the engine, then it would produce radio sources with powers greater than radio-loud quasars. Since the fraction of cooling gas that actually fuels the radio source is negligibly small, it is not clear why there should be a relationship between the average $\dot{M}$ for cooling flows on scales of tens of kpc and radio emission powered by an engine < 0.1 pc in size.

An alternative idea for the x-ray/radio coupling is one in which the gas in the center of the cluster is heated by cosmic ray electrons from the active galactic nucleus (e.g., Rosner and Tucker 1989; Rephaeli 1987; Bohringer and Morfill 1988) or by magnetic field reconnection (Soker and Sarazin 1988) which is then balanced by radiative cooling. Such a model can produce the observed excess of x-ray emission near the cluster centers without requiring a large inflow of gas from the outer regions (Sulkanen, Burns, and Eilek 1989). This quasistatic model is not in conflict with currently available data since Doppler measurements (using x-ray lines) of cooling inflows have not been performed. Stewart *et al.* (1984) have criticized this model as giving rise to a possibly unstable equilibrium in the cluster core. However, this instability may not be catastrophic, affecting the dynamics of only the inner $\approx$10–50 kpc of the cluster and allowing the remainder of the cluster to be in hydrostatic equilibrium (Rosner and Tucker 1989). This model has also been criticized from an energetics point of view. Typical radio luminosities of the sources in our sample are 10^{41-42} ergs/s, less than the observed x-ray luminosity excess at the cluster cores. However, it is the underlying bulk kinetic energy of the outflowing plasma that powers the nonthermal radio emission (via *in situ* particle acceleration) and heats the cluster gas. Since the efficiency of the heating process is believed to be much greater than that of particle acceleration (via damping of hydromagnetic waves; e.g., Eilek 1982), then the resulting x-ray luminosity is expected to be greater than the radio.

The observations reveal a clear excess of radio sources associated with cooling core clusters. However, the interpretation is still somewhat uncertain. Both the cooling inflow and cosmic-ray heating models merit further study. Further investigation of the origin of the optical emission lines in cooling cores may help to differentiate between these competing ideas (e.g., Heckman *et al.* 1989).

Another interesting result from this study is the propensity of steep spectrum radio sources affiliated with cooling core clusters. It has been known for some time that radio sources in rich clusters tend to have steeper spectra than those outside such clusters (Roland *et al.* 1976). Our results appear to refine this relationship to suggest that, at least for cD galaxies, a cooling core plays a role in steepening the spectrum. This can be easily understood within the confines of the cooling inflow model. Within the cooling core of a cluster (where the cooling time is less than a Hubble time), the pressure of the cooling gas exceeds that expected for a hydrostatic gas without a cooling flow (thermal pressure dominates for subsonic inflow and ram pressure dominates within the sonic radius for a transonic inflow). Thus, cooling core clusters have higher central pressures than noncooling cores as seen in Table II. As the radio plasma expands into the relatively high-pressure environment, it will tend toward confinement by the ambient gas. The better the confinement, the smaller the radio source (for a given bulk kinetic energy of the radio plasma) and the smaller the adiabatic expansion losses. Thus, such radio sources will lose more of their energy via synchrotron radiation. Such spectra will "age" and steepen with time (e.g., Kardashev 1962). Therefore, one might expect to find smaller and steeper spectrum sources in cooling cores than in noncooling cores as is observed.

As noted in Sec. III, most of the radio sources in cooling cores tend to have small ($\lesssim 1$ kpc) or nonexistent jets. Here, too, the environment may play a key role. Transonic cooling inflows, in particular, may provide appropriate conditions for jet disruption. At the sonic radius (typically < 1 kpc, but see Sulkanen, Burns, and Norman (1989) for larger radii in cooler inflows), the thermal pressure and temperature of the ambient gas change dramatically. Soker and Sarazin (1987) and Norman *et al.* (1988) have argued that such "pressure walls" could disrupt jets via fluid instabilities or via the generation of internal shocks, respectively. Sumi *et al.* (1989) have applied this idea, in particular, to the jets in A2029. Once disrupted, the jet material will likely be subsonic and, therefore, highly turbulent. The turbulent eddies can significantly broaden the radio plasma, producing diffuse lobes or tails that have only a vaguely collimated or bipolar appearance (see, e.g., numerical simulations in Norman *et al.* 1988). This picture may explain sources such as those in A1795 and 3C 338 in A2199.

The origin of the more amorphous, circularly symmetric outer structure seen in A2052, as well as M87 and 3C 84 (NGC 1275), is unclear. It may simply be radio plasma moving outward from the sites of jet disruption, decollimated, or scattered symmetrically by turbulence in the flow. Alternatively, these amorphous structures may be the product of high-energy election diffusion similar in nature to the halo sources in Coma (e.g., Willson 1975) and a few other clusters (e.g., Hanisch 1982). Diffusion models for these halo sources have been relatively successful (e.g., Jaffe 1977; Schlickeiser *et al.* 1987). The morphology and spectrum of the smaller amorphous sources look like a scaled-down version of the halo sources. To first order, relativistic electrons generated at the galaxy nucleus could diffuse out along roughly radial magnetic field lines that are frozen in by a cooling inflow. The outward propagation of the electrons may be impeded by interaction with the inflow, and thus may not reach the large-scale sizes seen in the halo sources (which in the case of Coma is in a noncooling flow cluster). Such a model appears to reproduce the radio surface-brightness profile for 3C 317 in A2052 (Sulkanen, Burns, and Eilek 1989).

Finally, it must be noted that although there is an important excess of radio sources in cooling cores, there is an equally important class of luminous radio galaxy that avoid cooling cores, the wide-angle tails. The presence of WATs in noncooling core clusters may demonstrate that mechanisms other than gas inflow from the cluster can generate relatively powerful, extended radio sources associated with centrally dominant galaxies (e.g., mass loss from stars in the galaxy; galactic cannibalism). The lack of a cooling core atmosphere may also permit these sources to grow to larger sizes than the relatively small radio sources in cooling cores. Alternatively, Sulkanen, Burns, and Norman (1989) have proposed that transonic cooling flows, with somewhat lower temperatures at the sonic radius, may actually exist for galaxies with WATs. The slightly lower outer cluster temperatures (factors of 2–4 less than those in cooling cores with observed x-ray excesses) may be consistent with the somewhat lower x-ray luminosities observed for WAT clusters (for example, note that L_x for A2634 which contains 3C 465 is one of the lowest in Table II). The cooler temperatures both lower L_x and effectively hide the observational signatures of a cooling flow. Such cooler cooling inflows also shift the sonic radius (and the "pressure wall") out to $\gtrsim 10$ kpc. This is the same scale size as the observed jet/tail transition in WATS. By postponing the jet disruption to larger distances (and lower pressure) from the galaxy nucleus, the WATs may be allowed to grow to overall larger sizes.

The radio properties of the remaining ≈ 70 Abell clusters with cD galaxies in the parent sample will be published in Paper II. This will help to expand the range of cluster types, radio morphologies, and radio powers examined for this class of optically dominant galaxy.

The author wishes to thank J.-H. Zhao for his help in reducing the VLA data on A2052, J. W. Moody and N. Duric for their assistance in calibrating the VLA data, S. Gordon and R. Price for their efforts with the *Einstein* x-ray data, and an anonymous referee for a suggestion regarding survival analysis statistics. I would also like to acknowledge productive conversations with M. Sulkanen, D. Sumi, F. Owen, and J. Eilek. This work was supported by NSF Grant No. AST-8611511 and a NASA ADP Grant.

REFERENCES

Abramopoulous, F., and Ku, W. (1983). Astrophys. J. **271**, 446.
Arnaud, K. A. (1988). In *Cooling Flows in Galaxies and Clusters*, edited by A. Fabian (Cambridge University, Cambridge), p. 31.
Arnaud, K. A. (1989). Private communication.
Arnaud, K. A., *et al.* (1987). Mon. Not. R. Astron. Soc. **227**, 241.
Auriemma, C., Perola, G. C., Ekers, R., Fanti, R., Lari, C., Jaffe, W. J., and Ulrich, M.-H. (1977). Astron. Astrophys. **57**, 41.
Baars, J. W. M., Genzel, R., Pauliny-Toth, I. I. K., and Witzel, A. (1977). Astron. Astrophys. **61**, 99.
Baum, S. A. (1987). Ph.D. dissertation, University of Maryland.
Baum, S. A., and Heckman, T. M. (1986). In *Radio Continuum Processes in Clusters of Galaxies*, edited by C. P. O'Dea and J. M. Uson (NRAO, Green Bank), p. 119.
Begelman, M. (1986). Nature **322**, 614.
Begelman, M. C., Blandford, R. D., and Rees, M. J. (1984). Rev. Mod. Phys. **56**, 255.
Bohringer, H., and Morfill, G. E. (1988). In *Cooling Flows in Galaxies and Clusters*, edited by A. Fabian (Cambridge University, Cambridge), p. 87.
Burns, J. O., Owen, F. N., and Rudnick, L. (1979). Astron. J. **84**, 1683.
Burns, J. O., Schwendeman, E., and White, R. A. (1983). Astrophys. J. **271**, 575.
Burns, J. O., and Ulmer, M. P. (1980). Astron. J. **85**, 773.
Burns, J. O., White, R. A., and Hough, D. H. (1981). Astron. J. **86**, 1.
Canizares, C. R., Clark, G. W., Jernigan, J. G., and Markert, T. H. (1982). Astrophys. J. **262**, 33.
Cowie, L. L., Hu, E. M., Jenkins, E. B., and York, D. G. (1983). Astrophys. J. **262**, 29.
Eilek, J. A. (1982). Astrophys. J. **254**, 472.
Eilek, J. A., Burns, J. O., O'Dea, C. P., and Owen, F. N. (1984). Astrophys. J. **278**, 37.
Fabian, A. C., Ed. (1988). *Cooling Flows in Galaxies and Clusters* (Cambridge University, Cambridge).
Fabian, A. C., Hu, E. M., Cowie, L. L., and Grindlay, J. (1981). Astrophys. J. **248**, 47.
Fabian, A. C., *et al.* (1985). Mon. Not. R. Astron. Soc. **216**, 923.
Feigelson, E. D., and Nelson, P. I. (1985). Astrophys. J. **293**, 192.
Feigelson, E. D., Wood, P. A. D., Schreier, E. J., Harris, D. E., and Reid, M. J. (1987). Astrophys. J. **312**, 101.
Hanisch, R. J. (1982). Astron. Astrophys. **116**, 137.
Heckman, T. M. (1981). Astrophys. J. Lett. **250**, L59.
Heckman, T. M. (1989). Astrophys. J. **338**, 48.
Heckman, T. M., Baum, S. A., van Breugel, W., and McCarthy, P. J. (1988). In *Cooling Flows in Galaxies and Clusters*, edited by A. Fabian (Cambridge University, Cambridge), p. 245.
Hu, E. M., Cowie, L. L., and Wang, Z. (1985). Astrophys. J. Suppl. **59**, 447.
Hunstead, R. W., Murdoch, H. S., and Shobbroak, R. R. (1978). Mon. Not. R. Astron. Soc. **185**, 149.
Jaffe, W. J. (1977). Astrophys. J. **212**, 1.
Johnstone, R. M., and Fabian, A. C. (1988). Mon. Not. R. Astron. Soc. **233**, 581.
Jones, C., and Forman, W. (1984). Astrophys. J. **276**, 38.
Joshi, M. N., Kapahi, V. K., and Bagchi, J. (1986). In *Radio Continuum Processes in Clusters of Galaxies*, edited by C. P. O'Dea and J. M. Uson (NRAO, Green Bank), p. 73.
Kardashev, N. S. (1962). Sov. Astron. **6**, 317.
Lindgren, B. W. (1962). *Statistical Theory* (MacMillan, New York).
Longair, M. (1981). *High Energy Astrophysics* (Cambridge University, Cambridge).
Mathews, W. G., and Bregman, J. N. (1978). Astrophys. J. **224**, 308.
Matthews, T. A., Morgan, W. W., and Schmidt, M. (1964). Astrophys. J. **140**, 35.
Merritt, D. (1984). Astrophys. J. **276**, 26.
Mushotzky, R. F., Holt, S. S., Smith, B. W., Boldt, E. A., and Serlemitsos, P. J. (1981). Astrophys. J. Lett. **244**, L47.
Mushotzky, R. F., and Szymkowiak, A. E. (1988). In *Cooling Flows in Galaxies and Clusters*, edited by A. Fabian (Cambridge University, Cambridge), p. 53.
Norman, M. L., Burns, J. O., and Sulkanen, M. E. (1988). Nature **335**, 146.
O'Dea, C. P., and Baum, S. (1986). In *Radio Continuum Processes in Clusters of Galaxies*, edited by C. O'Dea and J. Uson (NRAO, Green Bank), p. 141.
O'Dea, C. P., Owen, F. N., and Keel, W. C. (1986). Can J. Phys. **64**, 369.
Owen, F. N., Burns, J. O., and White, R. (1984). In *Clusters and Groups of Galaxies*, edited by F. Mardirossian, G. Giuricin, and M. Mezzetti (Reidel, Dordrecht), p. 295.
Owen, F. N., White, R. A., Hilldrup, K. C., and Hanisch, R. J. (1982). Astron. J. **87**, 1063.
Pedlar, A., Ghataure, H., Davies, H. B., Harrison, B., Perdy, R., and Crane, P. C. (1988). In *Cooling Flows in Galaxies and Clusters*, edited by A. Fabian (Cambridge University, Cambridge), p. 149.

Rephaeli, Y. (1987). Mon. Not. R. Astron. Soc. **225**, 851.
Roland, J., Hanisch, R. J., Veron, P., and Fomalont, E. (1985). Astron. Astrophys. **148**, 323.
Roland, J., Veron, P., Pauliny-Toth, I. I. K., Preuss, E., and Witzel, A. (1976). Astron. Astrophys. **50**, 165.
Romanishin, W. (1987). Astrophys. J. Lett. **323**, L113.
Rosner, R., and Tucker, W. H. (1989). Astrophys. J. **338**, 761.
Sarazin, C. L. (1986). Rev. Mod. Phys. **58**, 1.
Schlickeiser, R., Sievers, A., and Thiemann, H. (1987). Astron. Astrophys. **182**, 21.
Schwab, F. R. (1980). Proc. SPIE **231**, 18.
Slee, O. B., and Reynolds, J. E. (1984). Proc. ASA **5**, 516.
Soker, N., and Sarazin, C. L. (1987). Astrophys. J. **327**, 66.
Soker, N., and Sarazin, C. L. (1988). In *Cooling Flows in Galaxies and Clusters*, edited by A. Fabian (Cambridge University, Cambridge), p. 367.
Stewart, G. C., Canizares, C. R., Fabian, A. C., and Nulsen, P. E. (1984). Astrophys. J. **278**, 536.
Struble, M. F., and Rood, H. J. (1987). Astrophys. J. Suppl. **63**, 555.
Sulkanen, M. E., Burns, J. O., and Eilek, J. A. (1989). In preparation.
Sulkanen, M. E., Burns, J. O., and Norman, M. E. (1989). Astrophys. J. **344**, 604.
Sumi, D. M., Norman, M. L., Smarr, L. L., and Owen, F. N. (1989). Astrophys. J. (in press).
Thomas, P. A., Fabian, A. C., and Nulsen, P. E. (1987). Mon. Not. R. Astron. Soc. **228**, 973.
Tonry, J. L. (1985). Astron. J. **90**, 2431.
Valentijn, E. A. (1988). Astron. Astrophys. **203**, L17.
Valentijn, E. A., and Bijleveld, W. (1983). Astron. Astrophys. **125**, 223.
van Breugel, W., Heckman, T., and Miley, G. (1984). Astrophys. J. **276**, 79.
von Hoerner, S. (1974). In *Galactic and Extragalactic Radio Astronomy*, edited by G. L. Verschuur and K. I. Kellermann (Springer, Berlin), p. 353.
Wentzel, D. G. (1974). Annu. Rev. Astron. Astrophys. **12**, 71.
White, R. E., and Sarazin, C. L. (1987). Astrophys. J. **318**, 629.
Willson, M. (1970). Mon. Not. R. Astron. Soc. **151**, 1.
Zhao, J.-H., Burns, J. O., and Owen, F. N. (1989). Astron. J. **98**, 64.